Performance analysis of Terahertz planar antenna on Low-K polymer substrates

K. A. KARTHIGEYAN[a], E. MANIKANDAN[b,*], S. RADHA[a]
[a]*Department of ECE, SSN College of Engineering, Chennai – 603110, India*
[b]*School of Electronics Engineering(SENSE), Vellore Institute of Technology-Chennai Campus, Tamil Nadu 600127, India*

Polymers have high transmittance to THz and infrared frequencies which makes it as a better substrate for high-frequency antennas design. We have investigated different configurations of patch antenna operating at mid-infrared range frequencies with broadband operation on various low-k polymer substrates using FEM simulation. The frequency dependent conductivity and dielectric properties of the materials and their effects on radiation performance of the patch is studied numerically. The concept of capacitive feeding and Defective Ground Structure are utilized for making miniaturized antennas. And, the capacitive coupled feeding with partial ground plane obtained the 10dB impedance bandwidth more than 12% for various polymer substrates.

(Received August 9, 2019; accepted June 16, 2020)

Keywords: Terahertz, Antenna, Polymer, Flexible, Radiation, Dielectric

1. Introduction

From the history and development of Infrared detectors, after Norton [1], it can be stated that "All physical phenomenon in the range of about (0.1-1.0) eV can be proposed for IR detector". Infrared detector finds applications in many areas such as surveillance, imaging, medical applications, quality inspection, space applications etc. Recently, solar rectenna for infrared energy harvesting has been attracted in the research [2]. In the solar spectrum, most of the energy content is in the form of infrared (~50%) which is not utilized by the current photovoltaic technology. In IR spectrum, the part of the energy is absorbed or reflected back and remaining is reradiated to the earth surface particularly in atmospheric window of (7-14) μm [3]. This long wavelength mid-IR finds many applications such as energy harvesting, IR detector for the focal planar array in imaging and so forth applications in details.

Antoni [4] has explained different types of IR detectors and material performances on it. It is also possible to extend the operation of HgTe Quantum Wells from infrared to THz detector applications [5]. Recently antenna coupled bolometer [6], MOM diodes [7,8] are attracted the field of research due to their improved sensitivity and performance. In this work, patch antenna operating at the mid-infrared range is designed on polymer-substrates and numerically simulated using FEM tool.

Polymer based substrates are mainly used in flexible and stretchable electronics that includes Display devices, RF equipments (Filters, Waveguides), solar cells and so forth [9, 10]. Another advantage of using polymer substrate is that, it has compatibility with conventional CMOS fabrication processes.

At higher frequencies, metal exhibits frequency dependent conductivity and the dielectric properties of the polymers also vary with respect to frequency. So it is mandatory to understand the properties and many experiments have been conducted to determine the dispersive nature of the metal at IR & Optical frequencies [11, 12]. Similarly, the dielectric properties at terahertz frequencies are characterized at different ranges and done by many researchers [13]-[16].The contribution of bound electrons is generally neglected at microwave frequencies. But at optical and IR frequencies the bound electrons also contribute by means of intraband transitions [17]. B.heinz et.al clearly studied and discussed the non-Drude like behavior of intraband transitions in thin film metals at optical and IR frequencies [18]. In [19], a capacitive probe-fed technique is utilized for making a compact structure with broadband operation.

The main objective of this work is to make a simple and novel design of patch antenna operating at mid-infrared frequencies on polymer substrates for operating in a broadband range approximately from (24-28) THz. First, the properties of the dielectric and metal at infrared frequencies are studied from the literature and discussed in details. Two different configurations for compact designs are introduced and simulated numerically. The combined effect of these techniques to design a broadband antenna is studied numerically by FEM simulation.

2. THz properties of materials

2.1. Metal properties

In the design of THz systems, it is necessary to have an accurate model for finding the frequency dependent metal conductivity and dielectric properties at these frequencies. Modeling of THz components such as Antennas, filters and waveguide using CAD tools requires accurate characterization of materials because the smallest error in the value might affect the entire systems. It is sufficient that standard the Drude model theory is enough to predict the terahertz conductivity of copper metal at room temperature operation.

Polymers have high transmittance to the terahertz frequency range. These are mainly used as the base material in THz imaging, molecules detection, optical components, spectroscopic investigations etc. Polymers with low dielectric constant and loss tangent are considered as an optimal substrate for high-frequency antennas in THz communication applications.

The classical Drude model is used to calculate the frequency dependent conductivity of materials. The following are the general equations used to determine the conductivity with respect to frequency,

$$\sigma_D = \frac{\sigma_0}{1 + j\omega\tau} \tag{1}$$

where σ_0 is given by (2) and (3)

$$\sigma_0 = ne^2\tau / m \tag{2}$$

$$\sigma_0 = \omega_p^2 / 4\pi\omega_\tau \tag{3}$$

where ω is the angular frequency, n is the electron density, e is the electron charge, m is the electron mass, σ_0 is the DC conductivity and ω_p, ω_τ are the plasma and damping frequencies. The DC conductivity is determined from the scattering rate.

In [20], the frequency dependent conductivity of the material can be written as,

$$\sigma = \varepsilon_0\omega_p^2 /[\Gamma(1+\omega^2/\Gamma^2)] + i\varepsilon_0\omega_p^2\omega/[\Gamma^2(1+\omega^2/\Gamma^2)] \tag{4}$$

And with the condition of $\omega << \Gamma$ where Γ is the scattering rate, can be written as,

$$\sigma_R \approx \varepsilon_0\omega_p^2 / \Gamma \tag{5}$$

By Matthiessen's rule, $\Gamma = \Gamma_p + \Gamma_D$ $\Gamma / 2\pi$ is the sum of temperature dependent and independent terms dominated by phonons and lattice defects, respectively. For bulk Cu, at room temperature, is 8.33THz.

2.2. Dielectric material properties

The dielectric constant and loss tangent can be calculated from the index of refraction and extinction coefficient obtained at terahertz frequencies. By applying Fourier Transform techniques to the THz-TDS samples, the complex refractive index values of the material can be calculated as,

$$\tilde{n}(\omega) = n(\omega) + ik(\omega) \tag{6}$$

where $n(\omega)$ represents the dispersion of THz pulse due to the material and $k(\omega)$ denotes the extinction coefficient. From the complex refractive, the values of permittivity and loss tangent are being extracted as follows.

$$\varepsilon_c = \varepsilon' + i\varepsilon'' = n_c^2 = (n + ik)^2 \tag{7}$$

$$\varepsilon_r = n^2 - k^2 \tag{8}$$

$$\tan\delta = (2nk)/(n^2 - k^2) \tag{9}$$

Seven polymer materials are chosen as the substrate for this work and their dielectric properties are listed in table.1. All the above-mentioned polymers and their properties are based on the experimental data's obtained at terahertz frequencies from the literature. By utilizing the above equations, the dielectric characteristics of the materials are reported.

3. Design of patch antenna

3.1. Conventional patch design

The terahertz patch antenna operating at mid-infrared frequencies on a polymer substrate along with their dimensions are displayed in Fig. 1.

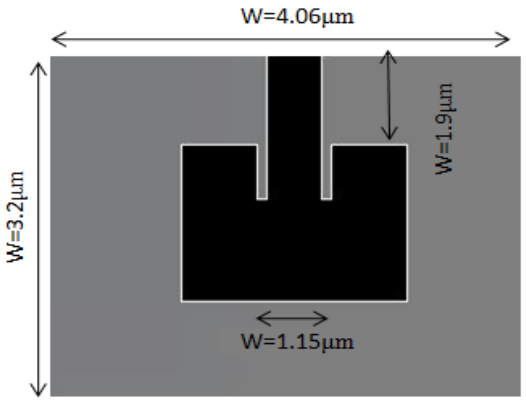

(a)

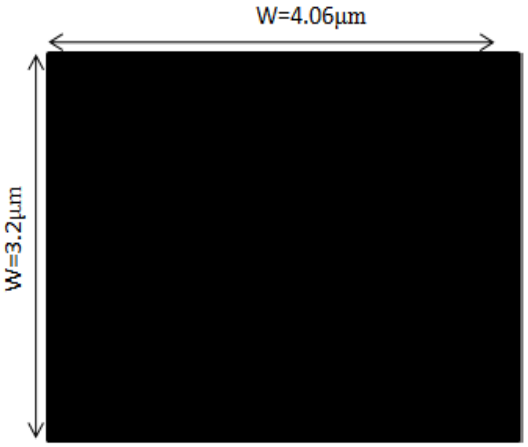

(b)

Fig. 1. Schematic of the terahertz patch antenna on polymer substrate a) Top view-patch layer b) Bottom view

By theory, the thickness of the patch should lie in the range of 0.003λ to 0.05λ. So, the thickness of the polymer dielectric substrate is kept as 0.5µm. Since, at terahertz frequencies the metals are not perfect conductors and becomes dispersive in nature, the patch and ground plane are replaced with copper material with the conductivity calculated using (4) and not a perfect electric conductor [20]. The skin depth value is calculated from (10),

$$\delta = \sqrt{\frac{\rho}{\pi f \mu}} \tag{10}$$

This is 0.013µm at 834cm^{-1} (25THz) for copper material. Hence, it is necessary to keep the thickness above the skin depth value and should be negligible compared to the substrate thickness for patch layer which is set to be 0.1µm. In this work, the structure is supposed to be maintained the same being substrate materials are changed with their permittivity varies from 2.5 to 3.25.

Table. 1. Dielectric properties of the polymer materials used

Substrate	Dielectric Constant ($\mathcal{E}_r$)	Loss Tangent (tanδ)	Resonant Frequency(THz)
ABS	2.8	0.03	26.4
Polyimide	3.25	0.021	24.19
Polycarbonate	2.61	0.027	27
PEEK	3	0.025	25.4
PDMS	2.5	0.05	28.8
PET	2.98	0.031	26.2
PLA	2.71	0.01	26

3.1.1. Conventional patch numerical simulation

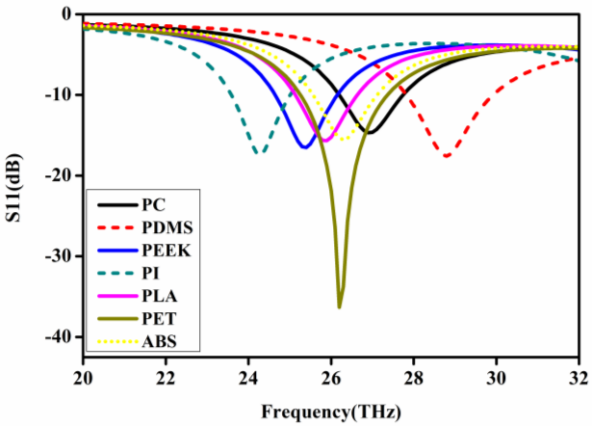

Fig. 2. Return loss and frequency response characteristics of the terahertz antenna on polymer substrates without DGS pattern (color online)

The width and length of the patch is calculated based on the design equations and the resonant frequency of the individual material varies accordingly. The resonant frequencies obtained by numerical FEM simulation best matches with the design analytical equations. The resonant frequency shift is noticed for Polyimide and PEEK substrate because of a small variation in feed width and length but the radiation characteristics show better performance at these frequencies.

Table 2. Simulation results for the conventional patch for polymer substrates at their individual resonant frequency based on the fixed geometries (F-Frequency, RL-Return loss, BW-Bandwidth)

Material	F(THz)	BW (%)	RL(dB)	Directivity(dB)	Radiation Efficiency (%)
ABS	26.3	5.73	15.55	6.02	58.06
PI	24.3	5.76	17.44	5.75	52.98
PC	26.9	5.57	14.68	6.17	59.69
PEEK	25.4	5.91	16.51	5.86	55.69
PDMS	28.8	7.29	17.57	6.3012	63.11
PET	26.2	8.21	36.3	5.77	55.53
PLA	25.9	5.79	15.65	5.95	56.96

The radiation characteristics of the conventional patch for different polymer substrates are shown in Table.2.The effect of dielectric properties of the polymer affects the

radiation performances. All the polymers used to have a lossy in nature at these frequencies and able to achieve reasonable efficiencies. But at their operating frequencies, all the substrates were achieved high directivity of greater than 5.55dB and a gain of more than 5dB.In general, the patch antenna supports narrowband operation (bandwidth of less than 3%) only, but for these low-k materials, THz patch achieves more than 5.5% and even 8.21% for PET substrate. PET and PDMS substrates are preferred more in flexible electronics.

The PDMS based patch has achieved an efficiency of 63.11% with the bandwidth of 7.29%. In all the cases, the patch and ground plane are replaced with a copper material instead perfect electric conductor (PEC). This is another main reason for the reduction in efficiency for the designed antennas. The radiation patterns of these configurations are unidirectional with high directivities.

3.2. Patch with defective ground structure

In patch antenna configuration, Defective Ground Structure (DGS) is involved in enhancing certain parameters of radiation characteristics [21-23]. DGS can also be utilized to create a compact structure resonating at the desired frequency [24-26]. In this work, an inverted U-shape slot is being introduced at the ground plane of the patch antenna and the corresponding simulated return loss characteristics are shown in Fig. 4. The observation here is at a particular width of 0.02λ, the resonant frequency of the patch is shifted towards left (minimum). The corresponding radiation characteristics are listed in Table 3. The DGS structure not only reduces the resonant frequency also the radiation efficiencies with an enhancement of 10dB impedance bandwidth.

Table 3. Radiation characteristics of the DGS based patch antenna for polymers substrate

Material	F(THz)	BW(%)	RL(dB)	Directivity(dB)	Radiation Efficiency(%)
ABS	15	8.7	29.45	3.21	34.915
PI	14.6	8.905	37.76	2.998	32.99
PC	16	8.125	24.25	3.31	34.8
PEEK	15.1	9.93	29.05	3.17	33.13
PDMS	15.2	8.55/7.78	20.81	3.48	40.27
PET	15.2	8.55	29.39	3.17	34.76
PLA	15.5	8.38	25.795	3.195	35.89

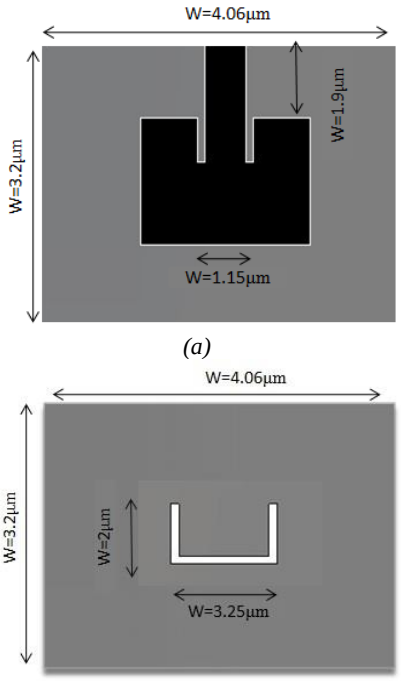

Fig. 3. Schematic of the terahertz patch antenna with DGS on polymer substrate a) Top view-patch layer b) Bottom view – DGS structure

3.2.1. Simulation result

The radiation patterns of the proposed DGS patch antenna are shown in Fig. 5. An introduction of a slot in the ground plane gives rise to a back lobe in the radiation patterns but no ripples could be seen in the patterns.

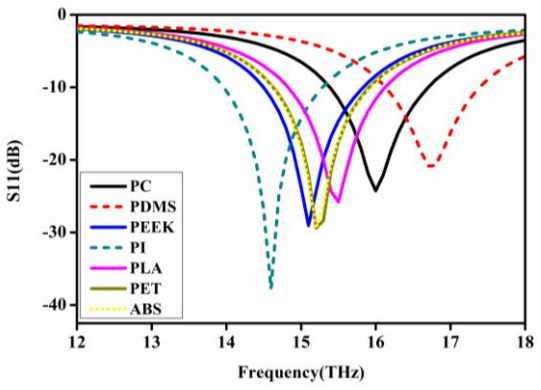

Fig. 4. Simulated return loss characteristics of the polymer based DGS patch antenna (color online)

Thus the DGS antenna is able to support bidirectional operations. On comparing, this PDMS based patch has good radiation characteristics with a broadband operation.

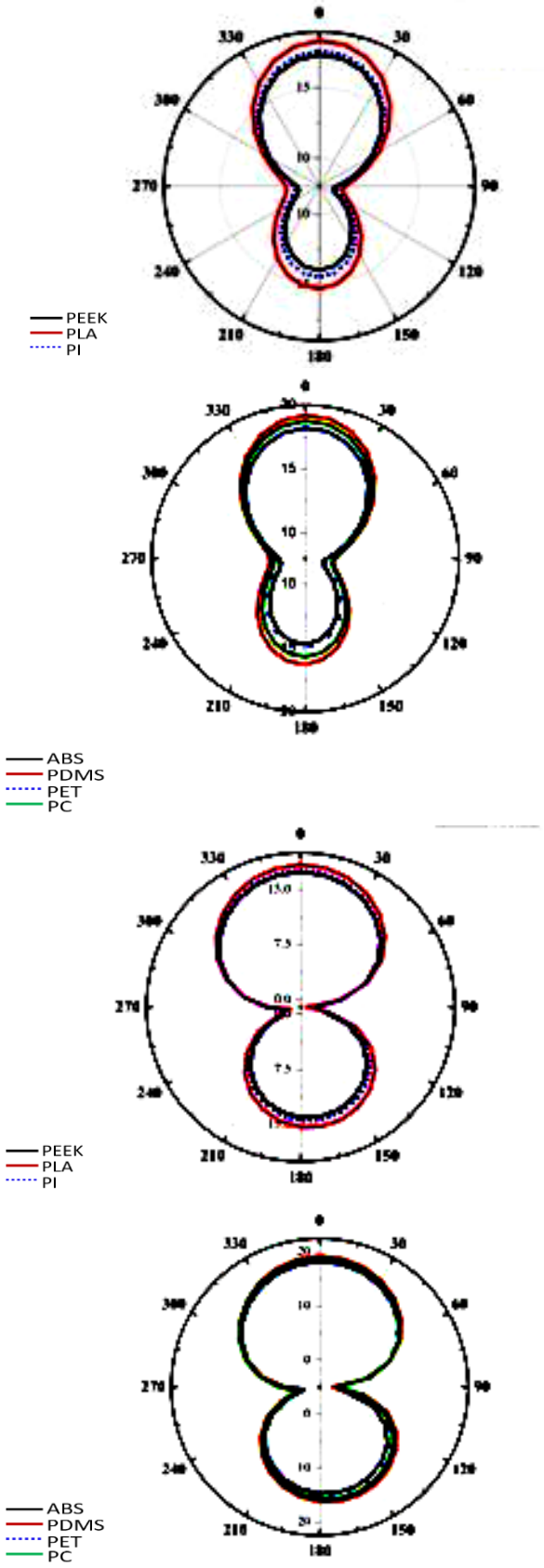

Fig. 5. Radiation Patterns for DGS patch antenna a,c)E-plane & H-plane for three substrates namely PEEK, PLA and PI b,d)E & H-plane for the four polymer substrates ABS, PDMS, PET and PC respectively (color online)

4. Patch antenna with modified feed (without DGS)

The schematic of the modified feed patch with the normal ground plane is shown in Fig. 6. This modified feeding allows designing a compact patch antenna without affecting the performance. This feeding is basically a parasitically coupled technique.

Table 4. Radiation characteristics of the Modified feed patch antenna (without DGS)

Material	F(THz)	BW (%)	RL(dB)	Directivity(dB)	Radiation Efficiency (%)
ABS	22.3	6.16	19.49	5.823	60.11
PI	20.8	4.22	13.73	5.484	56.12
PC	22.9	6.99	23.94	5.9793	61.37
PEEK	21.5	5.6	17.82	5.666	58.05
PDMS	24.1	7.9	34.18	6.266	64.31
PET	21.8	5.6	17.35	5.709	58.916
PLA	22	5.65	17.15	5.7565	59.77

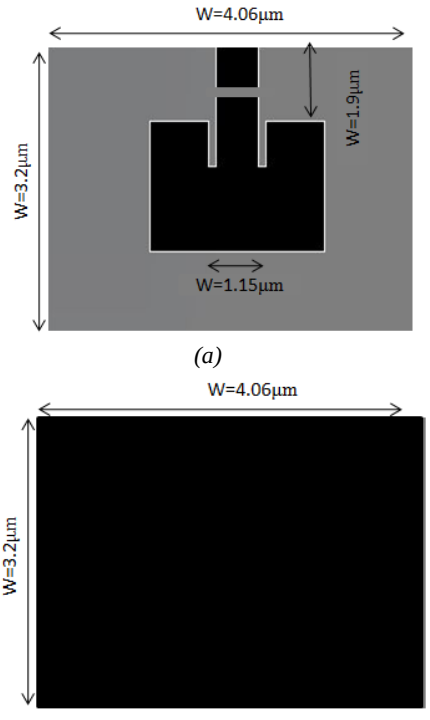

Fig. 6. Terahertz patch antenna with modified feed-Normal ground plane a) Top view-patch layer b) Bottom view

This parasitically coupled feeding allows the reduction of geometry size with better radiation characteristics. The radiation efficiency and the directivity is comparable to the conventionally designed antenna at their resonant frequencies. In this way, the size of the antenna at resonant frequencies listed in the table is reduced by (15×14) % of the original size. The bandwidth is also improved in a reasonable way without affecting the radiation performance.

4.1 Proposed modified feed patch with DGS

The introduction of a slot in the ground plane and feed make the resonant frequency shift towards left (Minimum).The DGS introduces back lobe behavior in the radiation pattern and thereby reducing radiation efficiency and directivity values. The slot in the feed also does the same thing but without affecting radiation characteristics. The observation is, the combination of DGS and parasitically coupled feeding enhancing the radiation at the desired resonant frequencies with broadband operation.

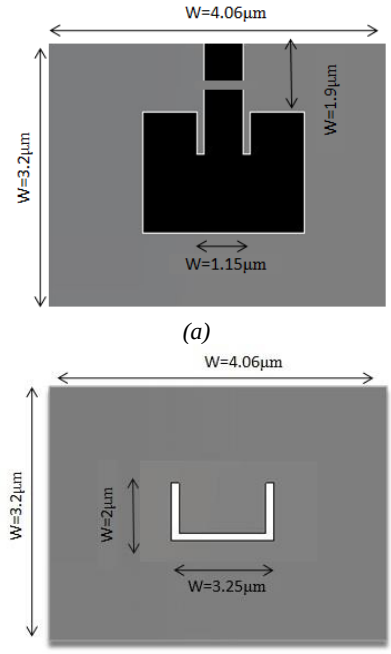

Fig. 7. Schematic of the proposed modified feed patch antenna with DGS structure a) Top view-patch layer b) Bottom view

The slots introduction generally induces a capacitive mechanism which is able to reduce the resonant frequency operation. The slots present in the ground plane diffracts the fields at the edges and the introduced back lobe operation is able to cancel out by a slit in the feed. The diffracted fields from edges are converted as a forward propagation and added to the patch radiation. Thus, this modified patch is able to resonate at their desired frequencies in a wider band with good radiation characteristics.

Table 5. Effect of slot in the feed and their radiation characteristics with DGS structure

Material	F(THz)	BW (%)	RL(dB)	Directivity(dB)	Radiation Efficiency (%)
ABS	26.6	12.08	25.81	3.8135	52.95
PI	24.4	11.54	16.77	3.8835	47.13
PC	27.4	11.85	27.83	3.9682	54.076
PEEK	25.7	12.12	20.27	3.8518	50.29
PDMS	28.6	12.29	25.25	3.9773	57.295
PET	26	11.63	19.08	3.6511	50.254
PLA	26.2	12.26	23.18	3.8908	51.818

From Table 5, it is observed that the bandwidth of operation is enhanced (more than 11%) with comparable radiation efficiency. But the directivity of the proposed antenna is slightly low compared to the conventional patch design. The return loss characteristics of the simulated proposed design are shown in Fig.8.It is evident that this concept supports broadband operation without affecting the resonant frequencies.

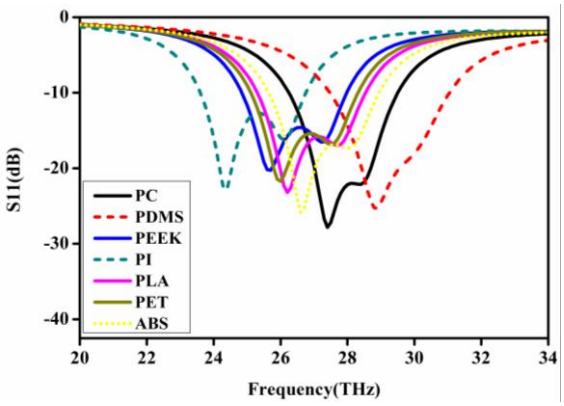

Fig. 8. Return loss characteristics of the proposed broadband polymer antennas (color online)

5. Features of this work

In this work, different polymer substrates and their dielectric properties are discussed. Based on the properties of the dielectric and copper metal, terahertz patch antenna is designed and its radiation performance characteristics are studied. Two different approaches namely DGS and parasitically coupled feeding is proposed for creating the compact structure and their characteristics are discussed as well. Next, the combination these techniques could enhance the broadband operation at their resonant frequencies with better radiation characteristics is obtained.

6. Conclusions

In this paper, the material properties at THz frequencies and their frequency dependent nature are studied and discussed in details. Two different techniques namely DGS and parasitically coupled feeding were utilized to create a compact patch design. The combined effect of parasitically coupled feeding with partial ground plane for patch antenna on different polymer substrates have been studied numerically. Compared to the originally designed patch, better radiation performances are observed for the proposed design with broadband operation. In summary, the PDMS substrate offers better performance in terms of bandwidth and radiation efficiency.

References

[1] Y. Radi, C. R. Simovski, S. A. Tretyakov, Physical Review Applied **3**, 037001 (2015).

[2] Wen-Chen Chen, Andrew Cardin, Machhindra Koirala et al., Opt. Express **24**, 6783 (2016).
[3] Jeremy A. Bossard, Lan Lin, Seokho Yun et al., ACS Nano **8**(2), 1517 (2014).
[4] Paul R. Norton, Proc. SPIE 3698, Infrared Technology and Applications **XXV**, 652 (1999).
[5] R. L. Bailey, ASME. J. Eng. Power **94**(2), 73 (1972).
[6] A. M. A. Sabaawi, C. C. Tsimenidis, B. S. Sharif, IEEE Journal of Selected Topics in Quantum Electronics **19**(3), 9000208 (2013).
[7] Antoni Rogalski, Infrared Physics & Technology **43**(3), 187 (2002).
[8] S. Dvoretsky, N. Mikhailov, Y. Sidorov et al., Journal of Elec. Mater. **39**, 918 (2010).
[9] K. Takebe, Y. Ikeshima, H. Miyashita, K. Takano, M. Hangyo S. S. Lee, Electronics Letters **50**(20), 1410 (2014).
[10] M. Bareib et al, IEEE Transactions on Microwave Theory and Techniques **59**(10), 2751 (2011).
[11] A. Kawakami, S. Saito, M. Hyodo, IEEE Transactions on Applied Superconductivity **21**(3), 632 (2011).
[12] Alexander Podzorov, Guilhem Gallot, Appl. Opt. **47**(18), 3254 (2008).
[13] M. Kubo, X. Li, C. Kim, M. Hashimoto, B. J. Wiley, D. Ham, G. M. Whitesides, Adv. Mater. **22**(25), 2749 (2010).
[14] S. Lucyszyn, The 11th IEEE International Symposium on Electron Devices for Microwave and Optoelectronic Applications, EDMO, p. 180, 2003.
[15] M. P. Kirley, J. H. Booske, IEEE Transactions on Terahertz Science and Technology **5**(6), 1012 (2015).
[16] V. V. Meriakri, D. S. Kalenov, M. P. Parkhomenko, S. Zhou, N. A. Fedoseev, American Journal of Materials Science **2**(6), 171 (2012).
[17] J. A. Hejase, P. R. Paladhi, P. P. Chahal, IEEE Transactions on Components, Packaging and Manufacturing Technology **1**(11), 1685 (2011).
[18] Muhammad Mumtaz, Ahsan Mahmood, Sabih D. Khan, M. Aslam Zia, Mushtaq Ahmed, Izhar Ahmad, Applied Spectroscopy **71**(3), 456 (2017).
[19] S. F. Busch, M. Weidenbach, M. Fey, M. et al., J. Infrared Milli Terahz Waves **35**(12),p. 993 (2014).
[20] M. A. Ordal, L. L. Long, R. J. Bell, S. E. Bell, R. R. Bell, R. W. Alexander, C. A. Ward, Appl. Opt. **22**(7), 1099 (1983).
[20] H.-G. Boyen, R. Gampp, P. Oelhafen, B. Heinz, P. Ziemann, Ch. Lauinger, St. Herminghaus, Phys. Rev. B **56**(11) 6502 (1997).
[21] Wen-Quan Cao, Qian-Qian Wang, Bang-Ning Zhang, Wei Hong, IET Microwaves, Antennas & Propagation **11**(7), 1003 (2017).
[22] N. Laman, D. Grischkowsky, Appl. Phys. Lett. **90**, 122115 (2007).
[23] D. Guha, M. Biswas, Y. M. M. Antar, IEEE Antennas and Wireless Propagation Letters **4**(1), 455 (2005).
[24] Y. J. Sung, M. Kim, Y. S. Kim, IEEE Antennas and Wireless Propagation Letters **2**(1), 111 (2003).
[25] A. K. Arya, A. Patnaik, M. V. Kartikeyan, IEEE Applied Electromagnetics Conference (AEMC), Kolkata, p. 1, 2011.
[26] B. K. Kanaujia, M. K. Khandelwal, S. Dwari et al., Wireless Pers. Commun. **91**(2), 661 (2016).

* Corresponding author: manikandan.e@vit.ac.in